

PROCEEDINGS OF SPIE

[SPIDigitalLibrary.org/conference-proceedings-of-spie](https://spiedigitallibrary.org/conference-proceedings-of-spie)

Photorefractive Properties Of $\text{KTa}_{1-x}\text{Nb}_x\text{O}_3$ In The Paraelectric Phase

Aharon Agranat, Victor Leyva, Koichi Sayano, Amnon Yariv

Aharon Agranat, Victor Leyva, Koichi Sayano, Amnon Yariv,
"Photorefractive Properties Of $\text{KTa}_{1-x}\text{Nb}_x\text{O}_3$ In The Paraelectric Phase,"
Proc. SPIE 1148, Nonlinear Optical Properties of Materials, (4 January 1990);
doi: 10.1117/12.962143

SPIE.

Event: 33rd Annual Technical Symposium, 1989, San Diego, United States

ABSTRACT

We report the growth of doped Potassium Tantalate Niobate (KTN) crystals, and the characterization of their photorefractive properties in the paraelectric region. First the Top Seeded Solution Growth Method is reviewed and the growth process of a KTN:Cu,V crystal is described. Results of diffraction efficiency measurements of photorefractive gratings in these crystals at the paraelectric phase, are then presented. These experiments show high diffraction efficiencies, and indicate the possibility of amplitude modulation of the gratings by an external field. Results showing fixation of the gratings when the sample is close to the phase transition temperature are also described.

1. INTRODUCTION

Potassium Tantalate Niobate (KTN), was one of the first materials in which the photorefractive (PR) effect was detected¹⁻³. However, although it is described in the literature as one of the most sensitive PR materials, very little was done both experimentally and theoretically to explore its potential as a storage medium for volume holography. As will be explained below the special PR properties of KTN are expected to emerge from the proximity of the working point temperature to the ferroelectric phase transition temperature T_c . In previous experiments the samples used were producing a large amount of stray light in the vicinity of T_c .⁴ It was therefore required to set the working point further away from T_c . In addition, these crystals were undoped and therefore required the use of comparatively short wavelength illumination for excitation. In what follows we report the growth of highly doped KTN crystals and preliminary results of measurements of their PR properties.

The chemical composition of KTN is given by $\text{KTa}_{1-x}\text{Nb}_x\text{O}_3$. It undergoes a ferroelectric (Cubic-Tetragonal) phase transition at a temperature T_c given approximately by

$$T_c = 8.5x \text{ [K]} \quad (1)$$

where x is the Nb concentration in % per mole. On cooling further below T_c , KTN undergoes two additional transitions: Tetragonal-Orthorhombic, and Orthorhombic-Rhombohedral. A full phase diagram of these phase transitions as a function of x is given in ref [5]. It should be noted that for $x < 30\%$ the ferroelectric phase transition is second order, and for $x > 30\%$ it is first order.

In the paraelectric region (for $T > T_c$) KTN is cubic and thus the electro-optic effect is quadratic, the electrically induced birefringence Δn is therefore given by

$$\Delta n = \frac{1}{2} n_o^3 g P^2 \quad (2)$$

where n_o is the index of refraction, g is the quadratic electro-optic coefficient, and P is the static (dc field induced) polarization, given in the linear region by

$$P = \epsilon_o(\epsilon - 1)E \quad (3)$$

The space charge induced PR effect in KTN can be described as follows: The incident illumination excites mobile charge carriers (e.g. electrons in the conduction band) in the crystal. These charge carriers are transported by either diffusion or drift and form a space charge spatially correlated with the incident

illumination. In the presence of an external electric field E_o , these spacecharge fields E_{sc} induce birefringence changes given by

$$\begin{aligned}\delta(\Delta n) &= \Delta n(E_{sc} + E_o) - \Delta n(E_o) \\ &= \frac{1}{2}n_o^3 g \epsilon_o^2 (\epsilon - 1)^2 (2E_o E_{sc} + E_{sc}^2)\end{aligned}\quad (4)$$

The amplitude of the first order diffraction grating is therefore given by

$$\delta(\Delta n) = n_o^3 g \epsilon_o^2 (\epsilon - 1)^2 E_{sc} E_o \quad (5)$$

In the vicinity of the phase transition the dielectric coefficient is very large. For $T-T_c=10K$ the dielectric coefficient is typically 10^4 - 10^5 . The induced birefringence, and hence the diffraction efficiencies are expected to be very high. In addition equation (5) reveals that the created space charge gratings are transformed into refractive index gratings only by the application of an external field. This fact opens the way for amplitude modulation of the PR grating. And finally, in the vicinity of the phase transition due to the increased plasticity of the crystal, we expect to observe fixation effects of the PR gratings. (Similiar to what was observed in Strontium Barium Niobate by Micheron et al⁶).

In section 2 we shall briefly describe the crystal growth method. We shall then present two preliminary sets of data for KTN:Cu,V in section 3.1, and for KTN:Cr,Fe in section 3.2. Finally we shall discuss in section 4 the potential of doped KTN crystals as PR materials.

2. CRYSTAL GROWTH

The crystals were grown by us using the Top Seeded Solution Growth (TSSG) method⁷⁻¹⁰. A schematic description of the growth system is presented in Figure 1. The system consists of two main assemblies: the furnace and the pulling apparatus.

- (a) The furnace is an Alumina cylinder with inner diameter of 9" and inner height of 9". It is heated by six Super Kanthal heating elements. The Platinum crucible is located at the center of the furnace and supported by a thin Alumina crucible. Maximum temperature of the furnace is 1650C and normal operating power is 1.2 kW at 1250C.
- (b) the pulling apparatus consists of an Alumina tube to which the seed is attached by platinum wires. The tube is connected through a concentric stainless steel inner tube to the rotation and pulling mechanism. The pulling rate can be controlled electronically between 0.225 mm/hr to 1mm/sec. The rotation rate is typically 20 rpm, and the rotation direction is reversed every 160 seconds. A stabilized air stream flows into the Alumina tube through the inner stainless steel tube at approximately 5 liter/min and cools the seed.

The main stages of the growth process are as follows:

- (a) *Preperation of the solution.* First a solution of the crystal constituents is formed, preferably using one of the constituents as the solvent. (In the case of KTN the solvent is K_2O).
- (b) *Seeding.* A cooled seed is then lowered until it touches the solution. The temperature at the touching point is set (by controlling the furnace heating rate, and the seed cooling rate), to be on the Liquidus curve of the solution. At this point the seed+solution system is at equilibrium. Growth does not occur and the seed is not dissolved by the solution. Note that at this stage the only potential nucleation site is the contact point between the seed and the solution, because the temperature of the rest of the solution is above the Liquidus. At this stage a rotation of the seed is started in order to maintain isotropy of the temperature, and to stir the solution.
- (c) *Crystal Growth.* After this equilibrium is reached a slow cooldown of the combined seed+solution system is started, (typically at 0.5 C/hr). In accordance with the development of the growth, crystal pulling

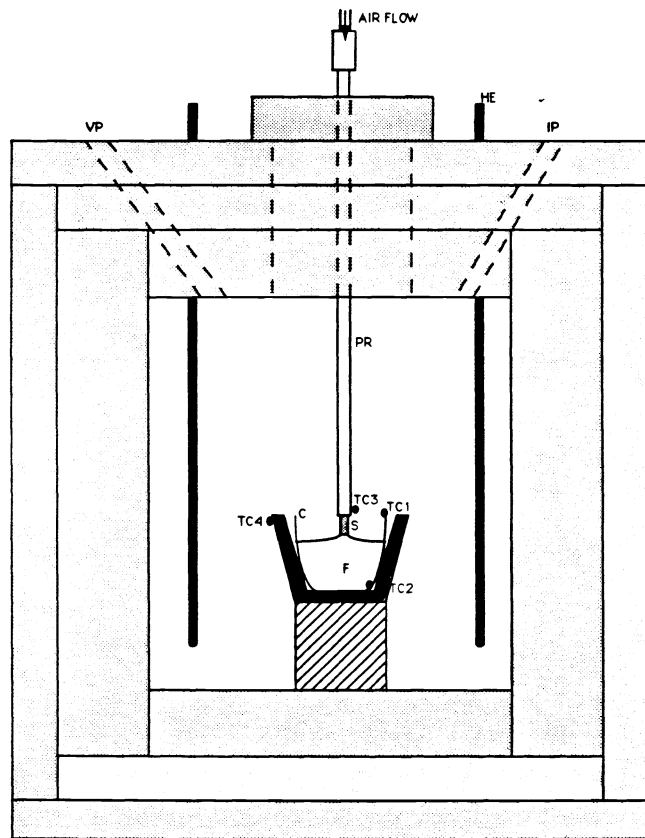


Figure 1. Crystal Growth System : VP-view port, HE-heating elements, IP- illumination port, PR- pulling rod, TC(1-4)-thermocouples, S-seed, C-crucible, F-flux

is started and continued until the crystal is completely out of the solution. (pulling starts typically 24 hours after the beginning of the growth (seeding)).

(d) *Annealing*: Finally the crystal is slowly cooled (typically 15-20 C/hr) to room temperature.

As an example we present the growth data of a KTN:Cu,V crystal:

(a) *Preparation of the solution*: The initial powder composition was as follows:

Material	% per mole
K_2CO_3	57
Ta_2O_5	22.8
Nb_2O_5	15.2
$2CuO$	2.5
V_2O_5	2.5

The powder was warmed up to 1300C and the resultant solution was soaked at that temperature for approximately 20 hours.

(b) *Seeding*. The seed was taken from a similar crystal. It was a rectangular prism 0.35x0.25x0.75 cm³ in size, and cut along the crystallographic [100] directions. The seeding temperature was determined to be at 1275C.

(c) *Growth in the solution*:

(1) Initial Cooldown: This is the main growth stage. The solution and seed were cooled together at 0.5 C/hr for 25 hours between 1275C and 1262.5 C.

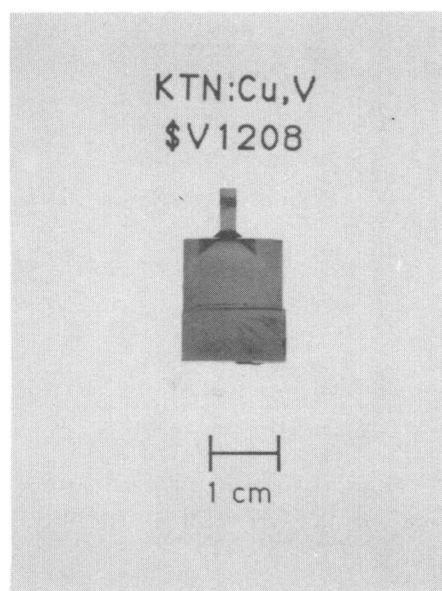
(2) Cooldown and Pulling. The crystal was then pulled at a rate of 0.225 mm/hr, while cooldown continued at 1.5 C/hr, for approximately 24 hours until the crystal emerged completely from the flux.

(d) *Annealing*: Finally the crystal was annealed to room temperature at 15 C/hr.

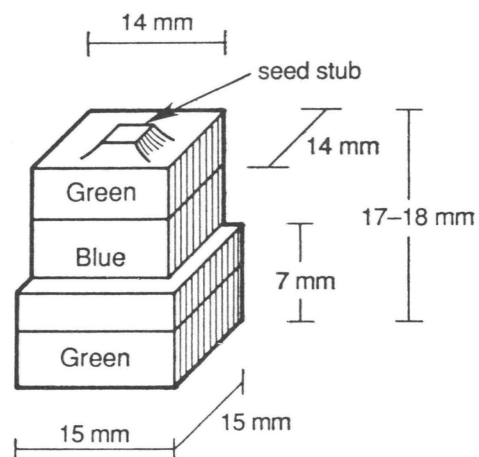
The resultant crystal is presented in Figure 2. It was blue-green and weighed 25.89 gm. Its chemical composition was determined by electron microprobe analysis and was found to be $KTa_{0.87}Nb_{0.13}O_3:Cu,V$. (The Cu concentration was 0-0.0024% per mole, and the V concentration was 0-0.0006 depending on the location of the sample). The optical quality was very good except for some external scratches.

3. EXPERIMENTAL RESULTS

In the following we describe experimental studies of the photorefractive properties of several KTN samples in the paraelectric phase. The diffraction efficiencies were measured using the experimental set-up described in Figure 3a. The samples were cut and polished along the crystallographic [100] directions, and were positioned relative to the writing beams as described in Figure 3b. The beams were aligned so that their bisector is orthogonal to the sample (i.e., in the z direction), and were polarized horizontally (in the x,z plane). The external electric field was applied in the x direction. The sample was mounted in a cryostat which enables a control of its temperature. The light source for the writing beams was an Ar⁺ ion laser operating at 514 nm. The diffraction efficiency was monitored by measuring the light diffracted by the crystal from either one of the writing beams, or from a probe beam generated by a He-Ne laser. The probe beam was aligned to match the Bragg condition for the PR grating. It was verified that its intensity was low enough not to have any noticeable effect on the crystal.

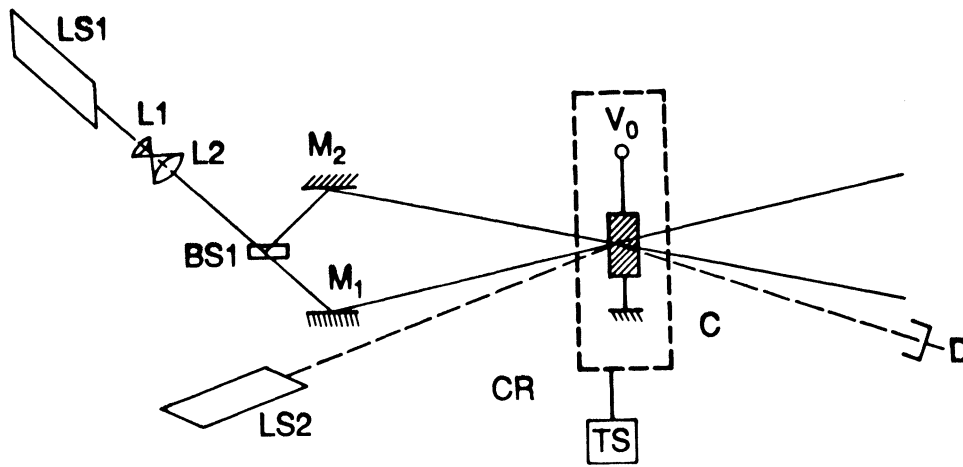


(a)

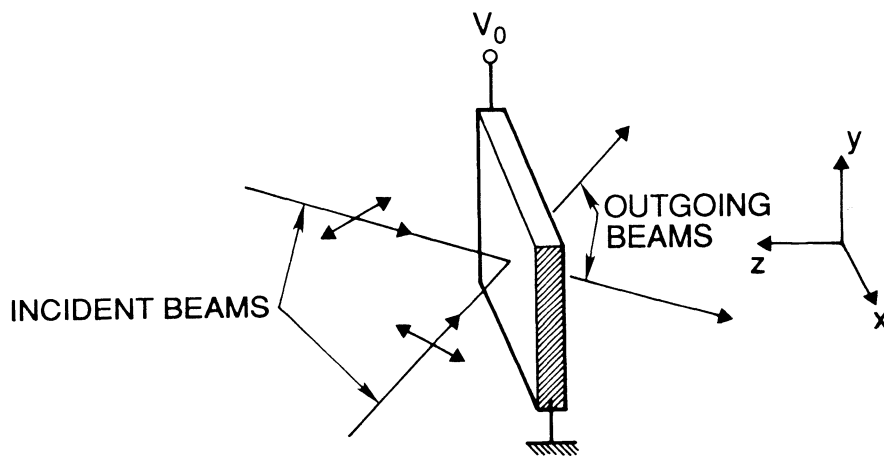


(b)

Figure 2. a) photograph of KTN:Cu,V crystal grown using the Top Seeded Solution Method b) dimensions and color of grown crystal



(a)



(b)

Figure 3. a) experimental setup LS1- Ar laser, LS2- HeNe laser, L1,L2- beam expansion lenses, BS1- beam splitter, M1,M2- mirrors, CR-cryostat, V_0 - bias voltage, D- detector b) orientation of writing beams

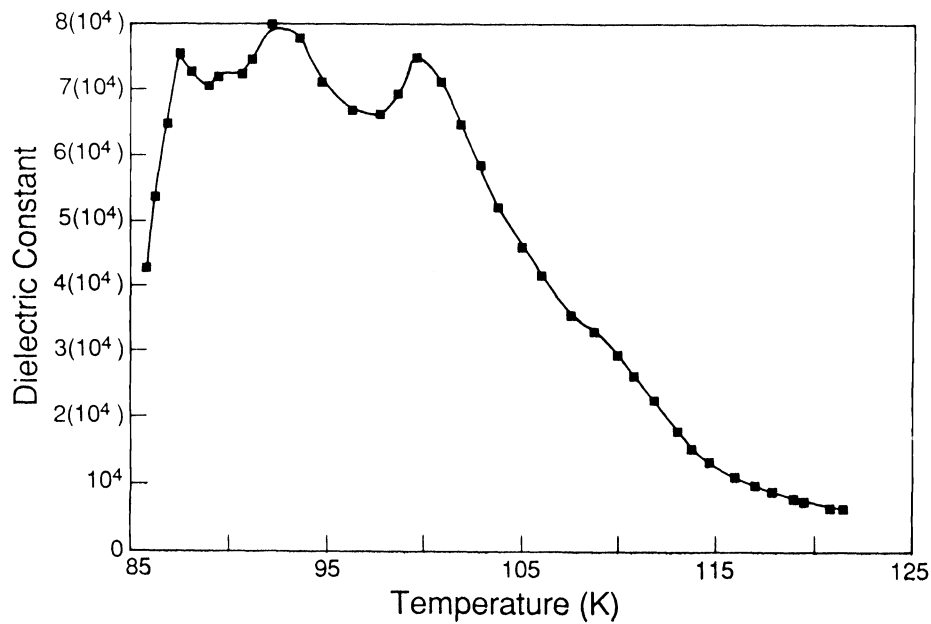


Figure 4. Low frequency (static) dielectric constant vs. temperature of KTN:Cu,V sample. Position of peaks roughly corresponds to phase transition temperatures.

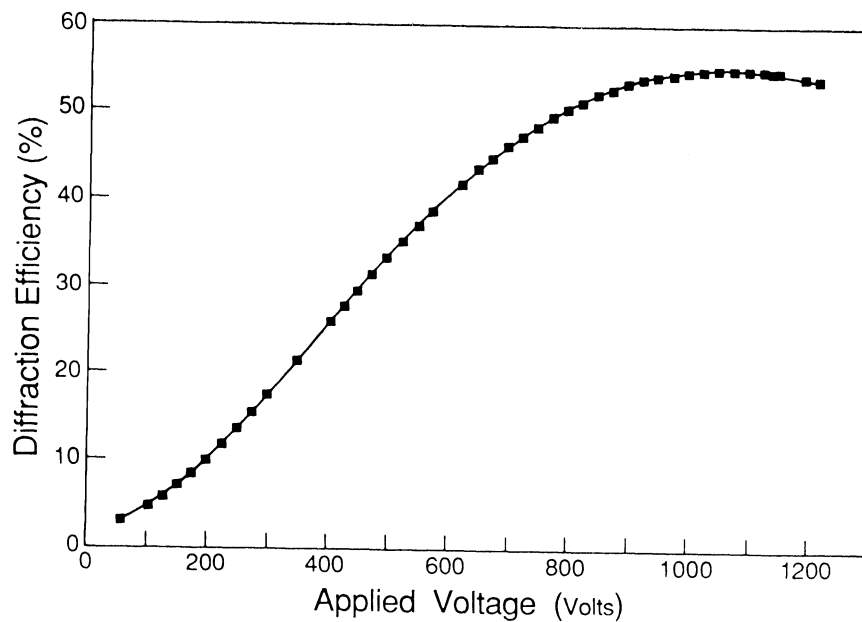


Figure 5. Diffraction efficiency of grating vs. applied voltage in KTN:Cu,V sample.

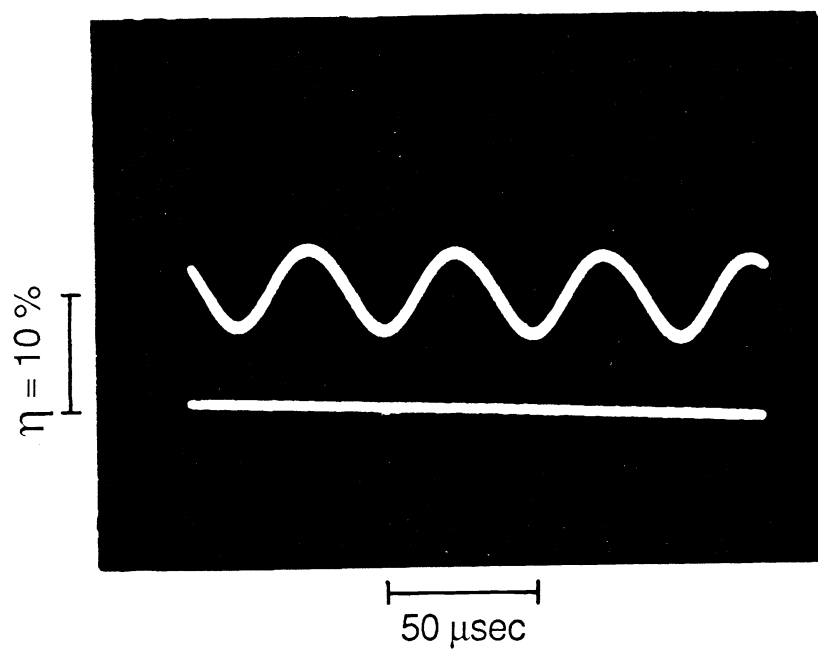


Figure 6. Modulated diffracted intensity with a 50 V/cm 20 kHz AC field and a 400 V/cm DC bias field applied to sample.

3.1 KTN:Cu,V

A KTN crystal doped with copper and vanadium was grown using the top seeded solution growth method. Its chemical composition was determined by electron microprobe analysis to be $\text{KTa}_{0.91}\text{Nb}_{0.09}\text{O}_3$. The dopants were below the detection limit of the probe. A $3 \times 3.5 \times 5 \text{ mm}^3$ sample was cut and polished along the [100] crystallographic axis, and was mounted in the system described in Figure 3 as explained above.

By measuring the capacitance, the low frequency (static) dielectric constant was determined as a function of temperature (figure 4). As the temperature is lowered the sample passes through the cubic, tetragonal, orthorhombic, and rhombohedral phases. The peaks in the dielectric constant correspond roughly to the phase transition temperatures. All photorefractive measurements were made in the cubic paraelectric phase at $T=112\text{K}$.

The diffraction efficiency, η , was measured using the experimental method described above. The writing beams were expanded to prevent unwanted spacecharge formation in the unilluminated regions of the sample. The writing beams intensity was 32 mW/cm^2 , and the exposure lasted 7.75 minutes. The beams intersected at an 11 degree angle. The applied electric field during writing was 900 V/cm . The diffraction efficiency as measured by monitoring the diffracted probe beam vs the applied electric field is presented in Figure 5. The diffraction efficiency increased with the field to approximately 60%, and saturated at $E_R=3 \text{ kV/cm}$. This saturation is discussed below. In addition the modulation of the diffracted light intensity by an ac electric field was demonstrated. A 50 V/cm ac field at 20kHz and a dc bias field of 400 V/cm were applied to the crystal. The temporal behavior of the diffraction efficiency is presented in Figure 6. The modulation frequency was limited to 20 kHz in this experiment by the bandwidth of the oscillator.

A second KTN:Cu,V $5 \times 4 \times 3 \text{ mm}^3$ sample was also grown and studied. The ferroelectric phase transition temperature is at $T_c=246\text{K}$. The absorption spectrum of the as grown crystal (Figure 7) contains a broad band centered at 680 nm . This is attributed to crystal field transitions of the Cu^{+2} ion. The sample in this state was weakly photorefractive ($\eta = .01 \%$ under a kilovolt bias field). The sample was then reduced by heating in a nominally pure Ar atmosphere at 800°C for 12 hours. Such a treatment in an oxygen deficient atmosphere induces oxygen vacancies.¹¹ The absorption spectra of the reduced sample is also shown in Figure 7. The band at 680 nm has disappeared indicating the transformation of the Cu^{+2} ion by way of the process $\text{Cu}^{+2} + e^- \rightarrow \text{Cu}^{+1}$. PR measurements were made in a manner similar to those done on the previously discussed sample. Two expanded beams, of equal intensity, from a 514 nm Ar^+ laser were incident on the crystal at an 11 degree angle. The sample was kept at a constant temperature of 251K by means of a thermoelectrically cooled mount within a vacuum chamber. A PR grating was then written for several seconds. One of the beams was then blocked by means of an electronic shutter. The diffraction of the remaining beam was then measured. The diffraction efficiency as a function of applied bias voltage for several intensities is given in Figure 8. The maximum diffraction efficiency was about 1% . The erasure time, defined as the time for the diffracted beam to decay from 90% to 10% of its initial value, is given in Figure 9 as a function of bias voltage for several intensities. The photoconductivity at room temperature was also measured (Figure 10). Its dependence was found to vary linearly with electric field but not with intensity.

3.2 KTN:Fe,Cr

A similar set of experiments was conducted on a KTN crystal doped with Iron and Chromium. The crystal was grown using the TSSG method, and was reduced in an Ar atmosphere after the growth. For the experiments a plate shaped sample, $7.8 \times 4 \times 1.2 \text{ mm}^3$ in size, was cut and polished along the crystallographic [100] directions. The ferroelectric phase transition temperature was determined from a capacitance vs. temperature measurement to be at $T_c=116\text{K}$.

The diffraction efficiency was measured using the following procedure: The sample was mounted in the system described in Figure 3. The sample was first exposed to the writing beams. Then one of the beams

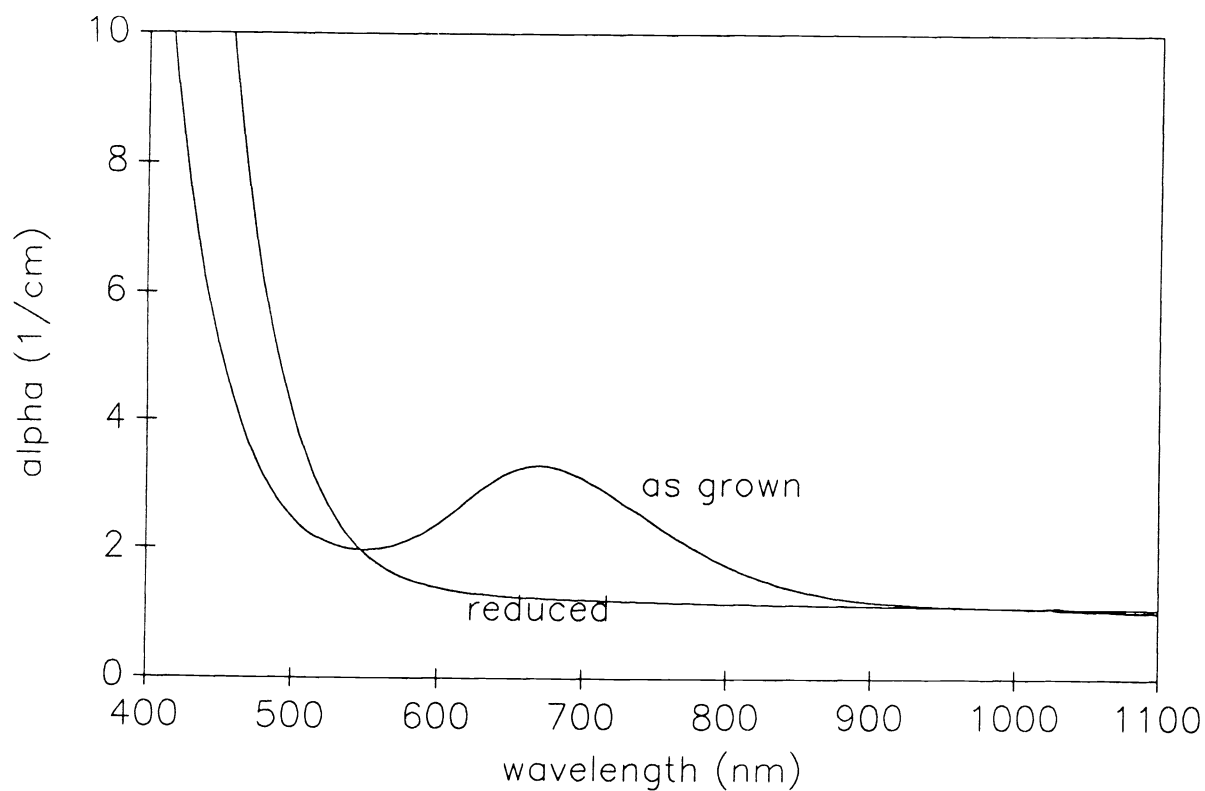


Figure 7. Absorption spectrum of as grown and reduced KTN:Cu,V crystal

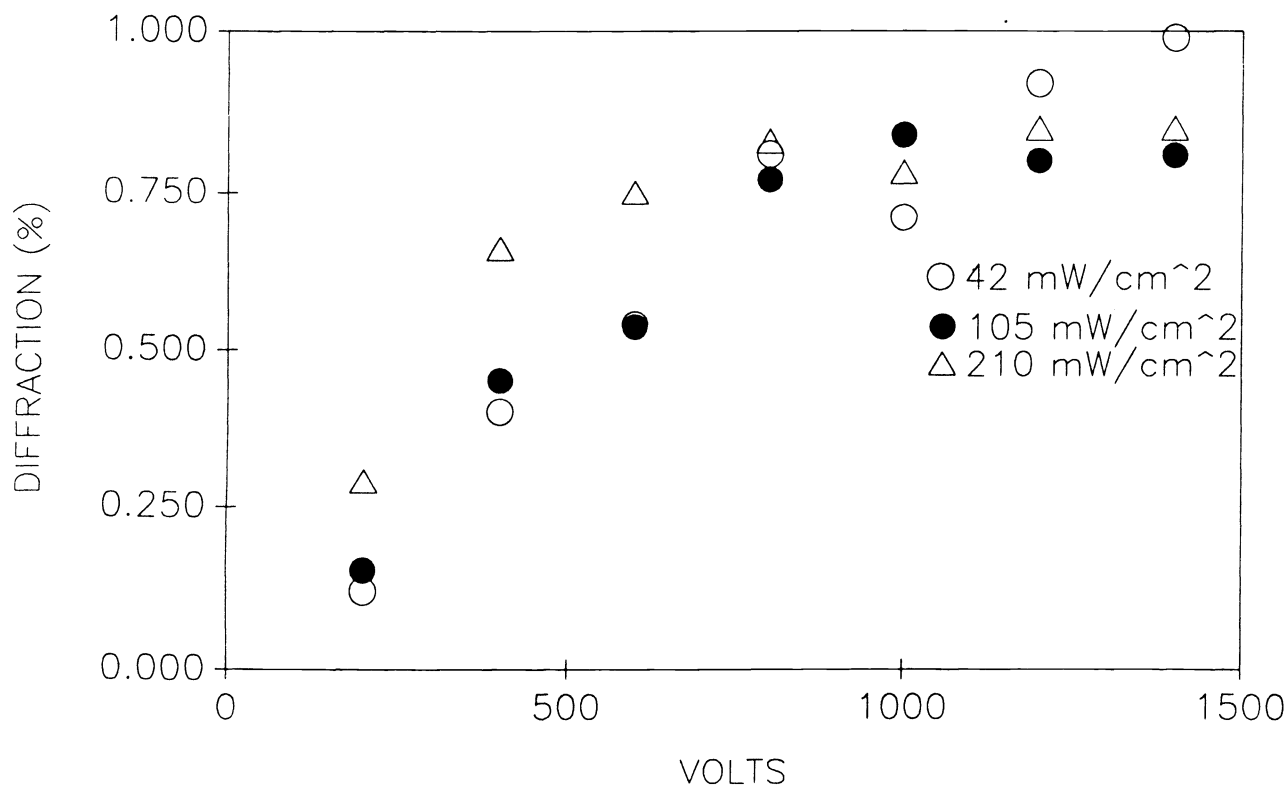


Figure 8. Diffraction efficiency of KTN:Cu,V sample vs voltage for several intensities

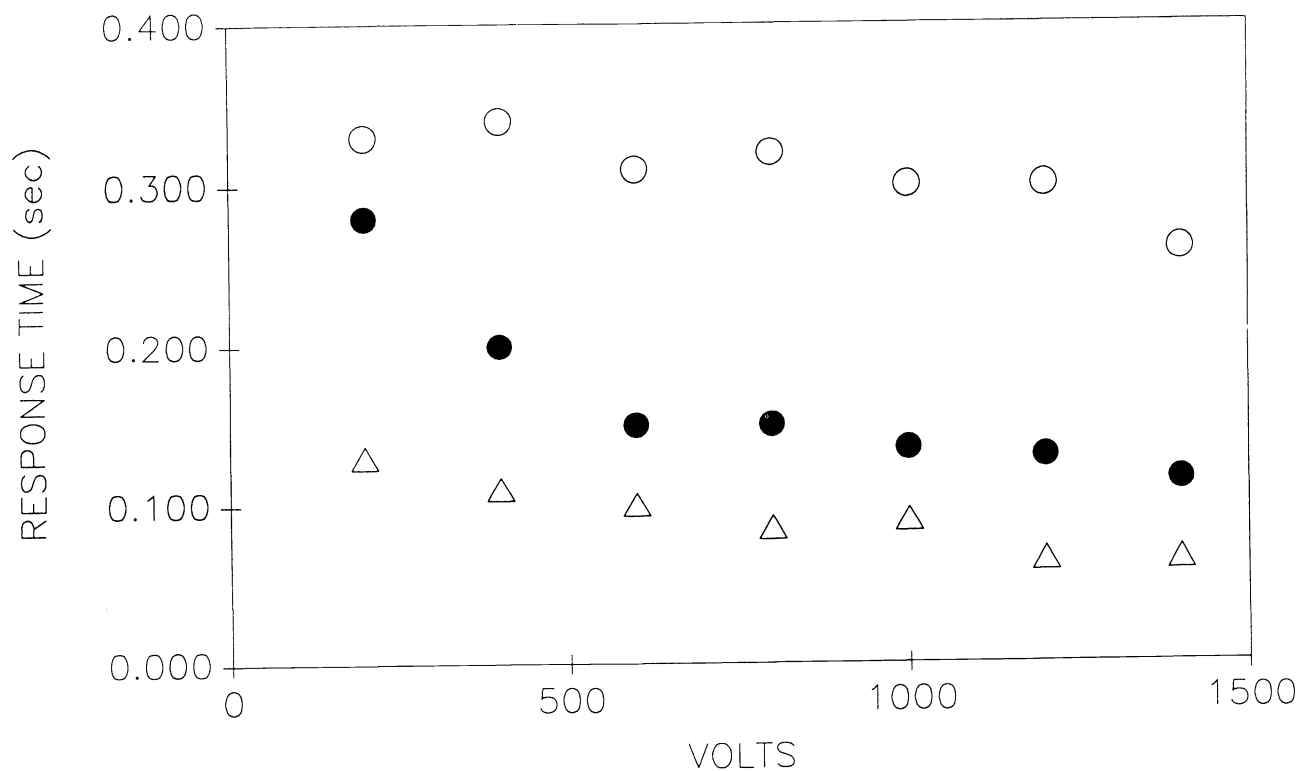


Figure 9. Erasure time of photorefractive grating vs bias voltage for several intensities.

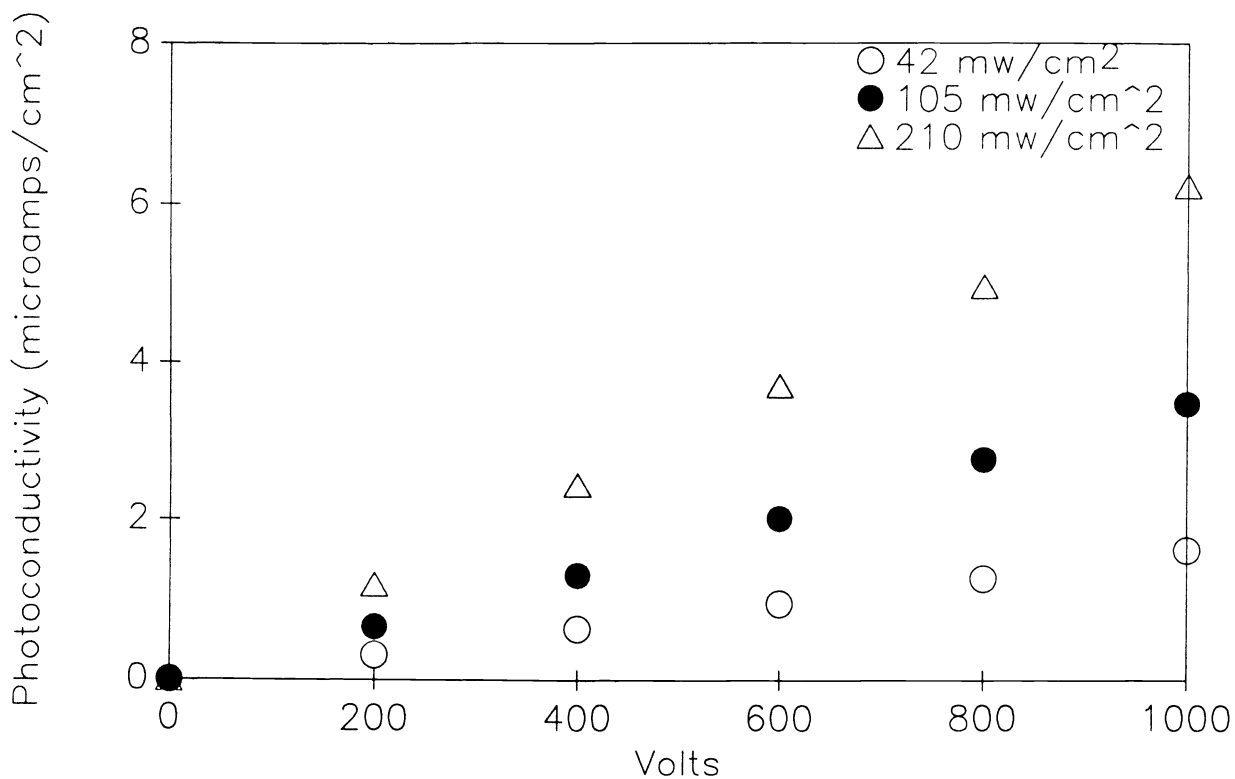


Figure 10. Photoconductivity vs applied voltage for several intensities.

was blocked and the light diffracted by the crystal from the other beam was monitored as a function of time and electric field.

The results of one set of measurements is presented in Figure 11a in terms of diffraction efficiency vs. time. The incident intensities were 8.05 mW and 6.37 mW respectively. The angle between the beams was 11.4 degrees. The experiment was performed at $T=120\text{K}$ and $V_o=500\text{V}$, as can be seen, the diffraction efficiency increased by approximately an order of magnitude during the first minutes of reading and reached a value of $\eta=6\%$. It then remained at this value for approximately 1 hour without decreasing significantly. The effect of the external field on η is presented in Figure 11b. As can be seen, although some hysteresis exists, the external field makes possible an efficient control of the grating's efficiency in KTN:Cr,Fe, similar to the KTN:Cu,V results in section 3.1.

A similar experiment was conducted at $T=127\text{K}$. Here the beams intensity was $I_1=I_2=2\text{mW}$ and the exposure time was 30 seconds. The results are present in Figure 12. The behavior is significantly different at this temperature. The diffraction efficiency first increases and then decays to zero.

4. DISCUSSION

The results presented in the last section clearly demonstrate the three important PR properties of doped KTN crystals; High diffraction efficiencies, Amplitude modulation of the PR grating by an external electric field, and fixation of the grating when operating close to T_c .

Let us consider the expected theoretical limits of these properties.

(a) **The limit of the diffraction efficiency:** The diffraction efficiency η is given by

$$\eta = e^{-\alpha l} \sin^2\left(\frac{\pi \delta(\Delta n) d}{\lambda \cos(\theta/2)}\right) \quad (6)$$

where $\delta(\Delta n)$ is the amplitude of the PR grating. The saturation of η , which appears in Figure 5, can be explained by the $\sin^2()$ dependence of η , or by the saturation of the static polarization under strong electric fields. For $\lambda=514\text{nm}$, $\theta=11$ degrees, $\alpha=1\text{cm}^{-1}$, $d=0.3\text{cm}$, and $\eta=60\%$ we get $\delta(\Delta n)=2.6(10^{-5})$, whereas under the same conditions for η_{max} we get $\delta(\Delta n)=3.7(10^{-5})$. This indicates that the dominant factor in saturating η is the saturation of $P(E)$ under strong electric fields. By measuring $P(E)$ independently, it was verified that this is in fact the case.¹²

(b) **The limit of the frequency response of the gratings amplitude modulation:** Here the limit is expected to arise from the critical slowing down of the dielectric response in the vicinity of the phase transition. This limit is expected to become effective at $f \approx 500\text{kHz}$.¹³

(c) **The fixing mechanism close to the phase transition:** Similar effects were observed by Micheron et al. in Strontium Barium Niobate crystals.⁵ They can be explained by assuming the formation of distortions due to impurity movements when the crystal is close to its phase transition temperature. These effects should be investigated further.

In conclusion: doped KTN crystals seem to be attractive for applications where large diffraction efficiencies, small erasure during readout, and amplitude modulation of the PR response are required. Careful selection of the dopants and working point temperature enable one to optimize the required property for the application.

5. REFERENCES

1. F.S. Chen, "A laser induced inhomogeneity of refractive indices in KTN", J. Appl. Phys., vol 38. p. 3418, 1967.

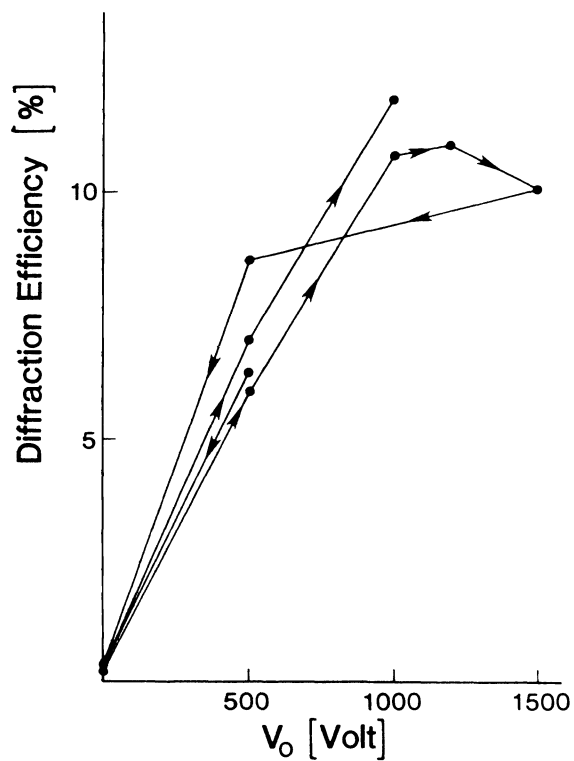
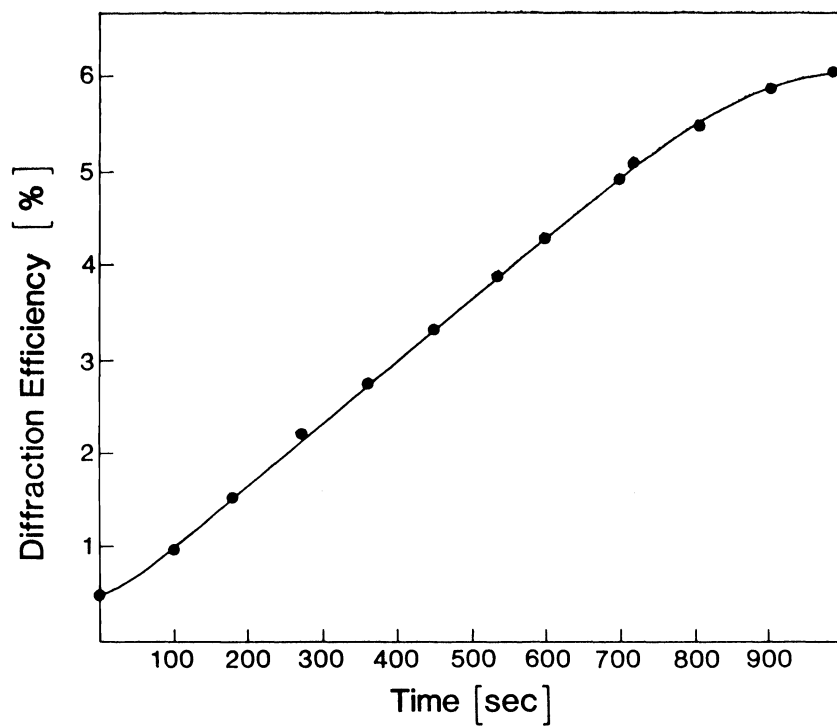


Figure 11. a) Diffraction efficiency vs time of readout for KTN:Fe,Cr sample at T=120K. b) Diffraction efficiency vs applied bias voltage for KTN:Fe,Cr sample.

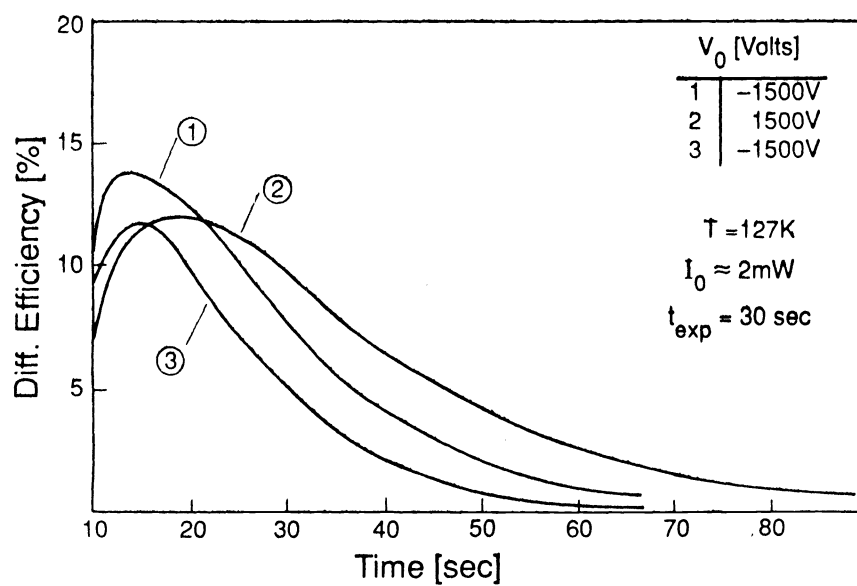


Figure 12. Diffraction efficiency vs time for sample at $T=127K$.

2. D. von der Linde, A.M. Glass, and K.F. Rodgers, "High- sensitivity optical recording in KTN by two-photon absorption", *Appl. Phys. Lett.*, vol. 26, pp. 22-24, 1975.
3. L.A. Boatner, E. Kratzig, and R. Orlowski, *Ferroelect.*, "KTN as a holographic storage material", vol. 27, p247, 1980.
4. R. Orlowski, L.A. Boatner, and E. Kratzig, *Opt. Comm.*, "Photorefractive effects in the cubic phase of Potassium Tantalate Niobate", vol. 35, p45, 1980.
5. C.M. Perry, R.R. Hayes, and N.E. Tornberg, in *Proceedings of the International Conference on Light Scattering in Solids*, M. Balkanski, ed. (Wiley, New York) p812, 1975.
6. F. Micheron and G. Bismuth, "Field and time thresholds for the electrical fixation of holograms recorded in $(\text{Sr}_{0.75}, \text{Ba}_{0.25})\text{Nb}_2\text{O}_6$ crystals", *Appl. Phys. Lett.*, vol. 22, pp71-72, 1973.
7. V. Belruss, J Kalnajs and A. Linz, "Top-seeded solution growth of oxide crystals from non-stoichiometric melts", *Matl. Res. Bull.*, vol. 6, pp.899-906, 1971.
8. P.A.C. Whiffin, J.C. Brice, "The Kinetics of the growth of $\text{KTa}_x\text{Nb}_{1-x}\text{O}_3$ crystals from solution in excess potassium oxide", *J. Crystal Growth*, vol. 23, pp. 25-28, 1974.
9. H.J. Scheel, P Gunther, "Crystal growth and electro-optic properties of oxide solid solutions", in *Crystal Growth of Electronic Materials*, Elsevier science Publishers, 1984.
10. W.A. Bonner, E.F. Dearborn, and L.G. Van Uitert, "Growth of potassium tantalate-niobate single crystals for optical applications", *Am. Ceram. Soc. Bull.*, vol 44[1], pp9-11, 1965.
11. W. Phillips and D.L. Staebler, "Control of the Fe^{+2} concentration in Fe doped lithium Niobate", *J. Elect. Matl.*, vol. 3, no 2. pp. 601-616, 1974.
12. A. Agranat, V. Leyva, A. Yariv, "Voltage controlled photorefractive effect in paraelectric $\text{KTa}_{1-x}\text{Nb}_x\text{O}_3:\text{Cu}, \text{V}$ ", to be published in *Opt. Lett.*, Oct. 1989.
13. M.E. Lines and A.M. Glass, "Principles and Applications of Ferroelectrics and Related Materials", Clarendon, Oxford 1977.